AMERICAN SOCIETY FOR MICROBIOLOGY | Infection and Immunity

Host-Microbial Interactions | Full-Length Text

Dectin-1/CARD9 induction of the TFEB and TFE3 gene network is dispensable for phagocyte anti-*Aspergillus* activity in the lung

Mariano A. Aufiero,[1] Neta Shlezinger,[2] Mergim Gjonbalaj,[3,4] Kathleen A. M. Mills,[5] Andrea Ballabio,[6,7,8] Tobias M. Hohl[1,3,4,5]

AUTHOR AFFILIATIONS See affiliation list on p. 12.

ABSTRACT Myeloid phagocytes of the respiratory immune system, such as neutrophils, monocytes, and alveolar macrophages, are essential for immunity to *Aspergillus fumigatus*, the most common etiologic agent of mold pneumonia worldwide. Following the engulfment of *A. fumigatus* conidia, fusion of the phagosome with the lysosome is a critical process for killing conidia. TFEB and TFE3 are transcription factors that regulate lysosomal biogenesis under stress and are activated by inflammatory stimuli in macrophages, but it is unknown whether TFEB and TFE3 contribute to anti-*Aspergillus* immunity during infection. We found that lung neutrophils express TFEB and TFE3, and their target genes were upregulated during *A. fumigatus* lung infection. In addition, *A. fumigatus* infection induced nuclear accumulation of TFEB and TFE3 in macrophages in a process regulated by Dectin-1 and CARD9. Genetic deletion of *Tfeb* and *Tfe3* impaired macrophage killing of *A. fumigatus* conidia. However, in a murine immune-competent *Aspergillus* infection model with genetic deficiency of *Tfeb* and *Tfe3* in hematopoietic cells, we surprisingly found that lung myeloid phagocytes had no defects in conidial phagocytosis or killing. Loss of TFEB and TFE3 did not impact murine survival or clearance of *A. fumigatus* from the lungs. Our findings indicate that myeloid phagocytes activate TFEB and TFE3 in response to *A. fumigatus*, and while this pathway promotes macrophage fungicidal activity *in vitro*, genetic loss can be functionally compensated in the lung, resulting in no measurable defect in fungal control and host survival.

KEYWORDS Fungus, Innate Immunity, Lung, TFEB, TFE3, Lysosome, *Aspergillus fumigatus*

Aspergillus fumigatus is a ubiquitous opportunistic mold that is the primary cause of invasive aspergillosis. *A. fumigatus* was recently classified by the World Health Organization as a pathogen of critical priority (1). Individuals with hematologic malignancies or those receiving high doses of corticosteroids often have quantitative and/or qualitative defects in innate immune function that render them susceptible to invasive disease upon inhalation of *A. fumigatus* conidia, the airborne infectious propagules (2). In the lungs of patients with defective innate immune function, conidia can germinate and form tissue-invasive hyphae that cause tissue injury and can result in mortality (3, 4). Due to challenges in early diagnosis, limited numbers of antifungal drug classes, and emerging resistance to front-line agents (5), overall mortality rates for patients with invasive aspergillosis remain high, with fungus-attributable rates of 20%–30% in high-risk groups (6). Thus, a better understanding of how the respiratory immune system responds to *Aspergillus* infection may lead to novel therapeutic strategies to improve patient outcomes.

Clearance of *Aspergillus* from the lungs is primarily mediated by innate immune phagocytes, including resident alveolar macrophages, recruited neutrophils, inflammatory monocytes, and monocyte-derived dendritic cells (Mo-DCs), all of which phagocytose and kill *Aspergillus* conidia before they can germinate in the lung (7, 8). Following

Editor Mairi C. Noverr, Tulane University, New Orleans, Louisiana, USA

Address correspondence to Tobias M. Hohl, hohlt@mskcc.org.

Andrea Ballabio is co-founder of CASMA Therapeutics and advisory board member of Next Generation Diagnostics and Avilar and Coave Therapeutics.

See the funding table on p. 12.

Received 2 June 2023
Accepted 22 September 2023

Published 20 October 2023

phagocytosis, the phagosome undergoes a maturation process *via* sequential fusion steps with components of the endocytic compartment, the final step of which is fusion with the lysosome, the primary degradative compartment of the cell (9). This maturation process and fusion with the lysosome allows for the acquisition of various antimicrobial factors and properties such as an acidified pH (*via* the vacuolar ATPase), the assembly of NADPH oxidase which produces antimicrobial reactive oxygen species (ROS), and the activation of lysosomal hydrolases which degrade phagosomal contents (10). Blocking these effector functions, such as by blocking phagosomal acidification with bafilomycin or abrogating ROS production by mutations in NADPH oxidase components, attenuates the ability of innate immune cells to kill *Aspergillus* (11–13).

The requirement for lysosomes in the clearance of phagocytic targets has long been appreciated, but it has only recently been understood how the lysosome can be dynamically regulated in cells. In the past decade, the transcription factors TFEB and TFE3 have been functionally characterized as master regulators of lysosomal biogenesis and autophagy in response to cellular stress (14–17). Various stimuli can lead to TFEB and TFE3 activation, including starvation, lysosomal damage, unfolded proteins, and infection (14). Activation of these transcription factors leads to lysosomal gene transcription and lysosomal biogenesis to enable the cell to cope with stress conditions. Bacterial pathogens or the fungal pathogen, *Candida albicans,* can activate these transcription factors in macrophages and promote downstream effector functions (18–20). In macrophages, inflammatory stimuli such as lipopolysaccharide (LPS) or bacteria promote lysosomal gene expression and the degradative capacity of lysosomes in a TFEB- and TFE3-dependent manner (18, 19). In turn, TFEB- and TFE3-activated lysosomes promote macrophage effector functions that enhance bacterial clearance (18). TFEB-regulated expression of *Irg1* and itaconate production contribute to macrophage antibacterial functions (21). TFEB and TFE3 can also directly regulate the expression of pro-inflammatory cytokines in cultured macrophages (19, 22). Thus, TFEB and TFE3 support macrophage effector functions in response to bacterial stimuli, but the *in vivo* role of TFEB and TFE3 during bacterial and fungal infection in mammalian hosts remains largely undefined, with no studies on microbial burden in infected organs or host survival.

In this study, we observed that *A. fumigatus* drives TFEB target gene transcription in infected neutrophils *in vivo* and nuclear localization of TFEB in macrophages *in vitro*. TFEB and TFE3 were required for optimal macrophage killing of *A. fumigatus in vitro* but were ultimately dispensable for lung leukocyte killing of *A. fumigatus* and murine survival during *A. fumigatus* respiratory infection in otherwise immune-competent mice.

RESULTS

Lysosomal genes are upregulated in lung neutrophils during *A. fumigatus* infection

We hypothesized that fungal engagement by myeloid phagocytes leads to the upregulation of genetic pathways that are important for their fungicidal activity. To identify which pathways are upregulated upon fungal engagement in the lung, we challenged mice with Alexa Fluor 633 (AF633)-labeled *A. fumigatus* conidia *via* the intratracheal route. Then, at 24 hours post infection (hpi) we isolated bystander ($AF633^{-}$), and fungus-engaged ($AF633^{+}$) neutrophils from the lung by FACS, and performed RNA-seq on sorted cells. Using the Kyoto Encyclopedia of Genes and Genomes (KEGG) pathway analysis, we compared genes that were upregulated in fungus-engaged neutrophils compared to bystander neutrophils. We found that genes associated with lysosomes were significantly overrepresented among all upregulated genes in fungus-engaged neutrophils (Fig. 1A).

The transcription factors TFEB and TFE3 control lysosomal gene expression in a variety of physiological contexts (14, 16, 23). We found that neutrophils express *Tfeb* and *Tfe3*, but not the other MiTF/TFE family members, *Mitf* and *Tfec* (Fig. 1B). In addition, *Tfeb* is upregulated upon fungal engagement (Fig. 1C), consistent with a known feed-forward

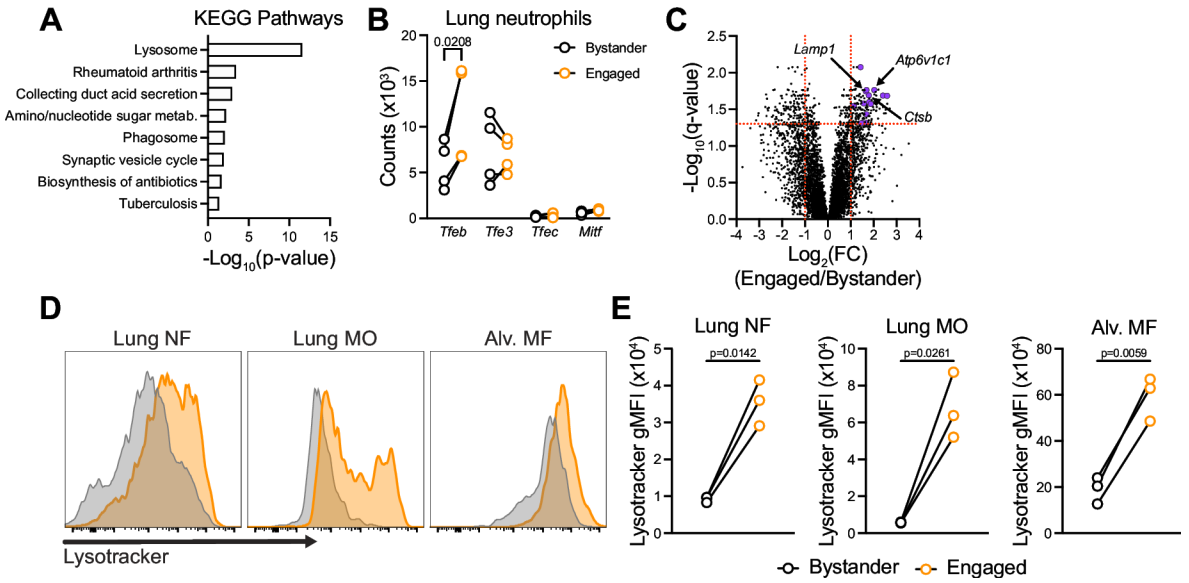

FIG 1 Fungus-engaged neutrophils upregulate lysosome genes, and lung phagocytes expand their lysosomal compartment in response to fungal engagement. (A) Bar chart displaying the statistically significant KEGG pathways of upregulated genes in engaged (AF633$^+$) neutrophils relative to bystander (AF633$^-$) neutrophils sorted from the lungs of *A. fumigatus* infected mice 24 hours post-infection. (B) Scatter dot plots indicating the gene counts for MiTF/TFE transcription factor family members. Dots represent independent experiments and lines link data from the same experimental replicate. (C) Volcano plot showing differential gene expression in engaged neutrophils relative to bystander neutrophils. Significantly upregulated TFEB target genes are colored purple. Vertical dashed lines indicate a $\log_2$ fold change of −1 or 1. Horizontal line indicates q-value = 0.05. (D) Representative histograms that display fluorescence intensity of LysoTracker in neutrophils (NF), monocytes (MO), and alveolar macrophages (Alv. MF) 24 hpi with AF633-labeled *Aspergillus*. The gray histogram indicates bystander phagocytes and the orange histogram indicates engaged phagocytes. (E) Scatter dot plots of the geometric mean fluorescence intensity of LysoTracker (D). Dots represent individual mice with lines depicting results obtained from bystander and fungus-engaged cells from the same mouse. (A, B, and C) Data are pooled from four independent experiments. (D and E) Data are representative of two independent experiments. Statistics: (B) Two-way RM ANOVA with Sidak's multiple comparisons test. (E) Paired *t*-test.

loop in TFEB activity (24). When compared to a published list of confirmed TFEB target genes (25), 15 confirmed TFEB target genes were significantly upregulated (see Table S1 for a list of genes) in fungus-engaged neutrophils, and no TFEB target genes were significantly downregulated (Fig. 1C).

In addition to neutrophils, alveolar macrophages, monocytes, and Mo-DCs phagocytose and kill conidia during *A. fumigatus* infection (7, 11). To assess whether fungal engagement led to an expansion of lysosomes in lung phagocytes, we challenged C57BL/6J [wild type (WT)] mice with AF633-labeled conidia, and stained lung cells *ex vivo* with LysoTracker, a fluorescent dye that labels lysosomes, at 24 hpi. Fungus-engaged neutrophils had increased LysoTracker signal compared to bystander neutrophils, consistent with an expansion of their lysosomal compartment (Fig. 1D). In addition, we observed a similar increase in LysoTracker signal in fungus-engaged lung monocytes and engaged alveolar macrophages compared to bystander cells. These data indicate that myeloid phagocytes expand their lysosomal compartment when cells engulf *Aspergillus* conidia in the lung.

A. fumigatus conidia activate TFEB and TFE3 in macrophages in part through C-type lectin receptors

Bacteria and *C. albicans* can activate TFEB and TFE3 in macrophages (19, 20, 22), although the mechanism by which fungal recognition is coupled to TFEB and TFE3 activation has not been defined. To test whether *A. fumigatus* could activate TFEB and TFE3, we challenged immortalized bone marrow-derived macrophages (iBMDMs) with *A. fumigatus* heat-killed swollen conidia and assessed nuclear translocation of endogenous TFEB and TFE3 by confocal microscopy, as previously described (19). We observed rapid

TFEB and TFE3 nuclear localization following *A. fumigatus* infection, which peaked at 1 hpi for TFE3 and at 4 hpi for TFEB. The nuclear to cytoplasmic ratio of TFEB and TFE3 returned to baseline levels by 24 hpi (Fig. 2A and B; Fig. S1A).

Phagocytes sense *A. fumigatus* through C-type lectin receptors that bind to fungal cell wall components (e.g., Dectin-1 binds fungal β-glucan), which then signals through spleen tyrosine kinase (Syk) to activate the adaptor protein Card9 to initiate a pro-inflammatory gene expression program (12). To test whether this pathway would also contribute to TFEB and TFE3 activation in response to *A. fumigatus* conidia, we challenged primary BMDMs from *Clec7a*$^{-/-}$ (i.e., the gene that encodes Dectin-1) and *Card9*$^{-/-}$ mice with *A. fumigatus* conidia and quantified TFEB nuclear translocation. We observed that both *Clec7a*$^{-/-}$ and *Card9*$^{-/-}$ BMDMs had a reduction in TFEB nuclear translocation following stimulation with *A. fumigatus* conidia compared to WT cells (Fig. 2C and D). Similar to TFEB, TFE3 nuclear translocation was reduced in *Card9*$^{-/-}$ BMDMs in response to challenge with *A. fumigatus* conidia (Fig. S1A and B). However, there was residual induction of TFEB and TFE3 nuclear trafficking compared to unstimulated cells, suggesting that additional signals may contribute to TFEB and TFE3 activation in response to *A. fumigatus*. These data suggest that challenge with *A. fumigatus* is sufficient to activate TFEB and TFE3 in phagocytes and that Dectin-1/CARD9 signaling is required for this process.

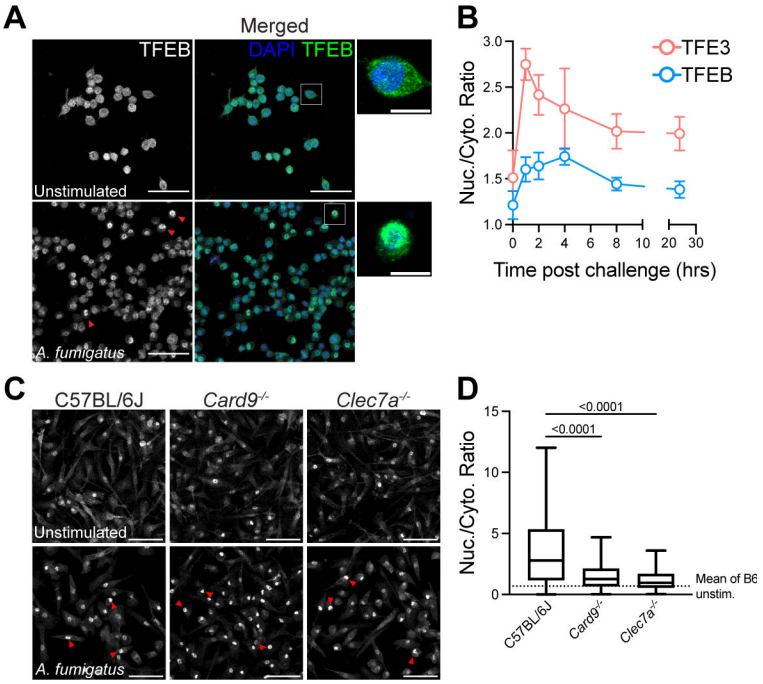

FIG 2 *A. fumigatus* conidia activate TFEB and TFE3 in macrophages *via* C-type lectin receptors. (A) Representative confocal micrographs of iBMDM cells stimulated with swollen heat-killed *A. fumigatus* conidia. Red arrowheads indicate cells with nuclear translocation of TFEB. The insets show high-magnification images of iBMDMs marked by the white square in representative fields. (B) Quantification of TFEB and TFE3 nuclear to cytoplasmic ratio displayed as mean ± SEM from (A). (C) Representative confocal micrographs of BMDM cells from B6, *Card9*$^{-/-}$, and *Clec7a*$^{-/-}$ mice at 2 hours post-challenge with *A. fumigatus* swollen heat-killed conidia. Red arrowheads indicate cells with nuclear translocation of TFEB. (D) Quantification of TFEB nuclear to cytoplasmic ratio displayed as a box and whiskers plot (C). Scale bar: 50 µm or 10 µm for the insets. Data are representative of two independent experiments. Statistics: Kruskal-Wallis test and Dunn's multiple comparisons test.

TFEB and TFE3 promote macrophage fungicidal activity *in vitro*

TFEB and TFE3 can drive the expression of immune genes in macrophages (19, 22) and activation of TFEB can enhance the bactericidal activity of macrophages (18). Furthermore, lysosomes are essential for the elimination of phagocytosed fungi (20). We hypothesized that TFEB and TFE3 would promote the fungicidal activity of phagocytes. To test this, we generated BMDMs from mice with *Tfeb* deficiency in hematopoietic cells (*Vav-iCre Tfeb*$^{f/f}$*; Tfeb*$^{\Delta hem}$) since global deletion is embryonic lethal (26). We also generated primary BMDMs from littermates with global *Tfe3* gene deletion (*Tfeb*$^{f/f}$ *Tfe3*$^{-/y}$; TFE3 KO) or from littermates that lacked *Tfeb* in hematopoietic cells as well as *Tfe3* in all cells (*Vav-iCre Tfeb*$^{f/f}$ *Tfe3*$^{-/y}$; DKO^{hem}). We confirmed successful TFEB depletion in BMDMs by Western blotting (Fig. S2A) and in circulating monocytes and neutrophils by flow cytometry (Fig. S2B). BMDMs from DKO^{hem} mice had a reduction in the transcription of two TFEB target genes, *Ctsb* and *Atp6v1c1*, that were upregulated in our lung neutrophil RNA-seq data set (Fig. S2C), providing further evidence that TFEB and TFE3 were successfully deleted. At baseline, we observed a modest increase in LysoTracker staining in BMDMs from DKO^{hem} mice compared to BMDMs from *Tfeb*$^{f/f}$ mice. This result indicates that loss of TFEB and TFE3 does not affect lysosomal acidification prior to BMDM challenge with *A. fumigatus* conidia (Fig. S2D and E). Next, we challenged BMDMs generated from DKO^{hem} or *Tfeb*$^{f/f}$ mice with FLuorescent *Aspergillus* REporter (FLARE) conidia that are surface-labeled with AF633 and encode RFP, as previously described (27). Upon phagocyte-mediated fungal killing, *Aspergillus* RFP fluorescence is quenched while AF633 fluorescence is preserved, enabling us to quantify the rate of fungal phagocytosis and fungal viability in diverse phagocyte subsets. The rate of conidial phagocytosis is measured by quantifying total AF633$^+$ events for each phagocyte subset analyzed (Uptake = Gate R1 + Gate R2; Fig. 3A). Fungal killing by a specific leukocyte subset is expressed as the frequency of leukocytes that are RFP$^+$ and AF633$^+$ divided by all AF633$^+$ leukocytes of the same subset independent of RFP fluorescence (i.e., all fungus-engaged leukocytes; fungal viability in a leukocyte subset = R1/[R1 + R2], Fig. 3A). *In vitro*, we did not observe any difference in

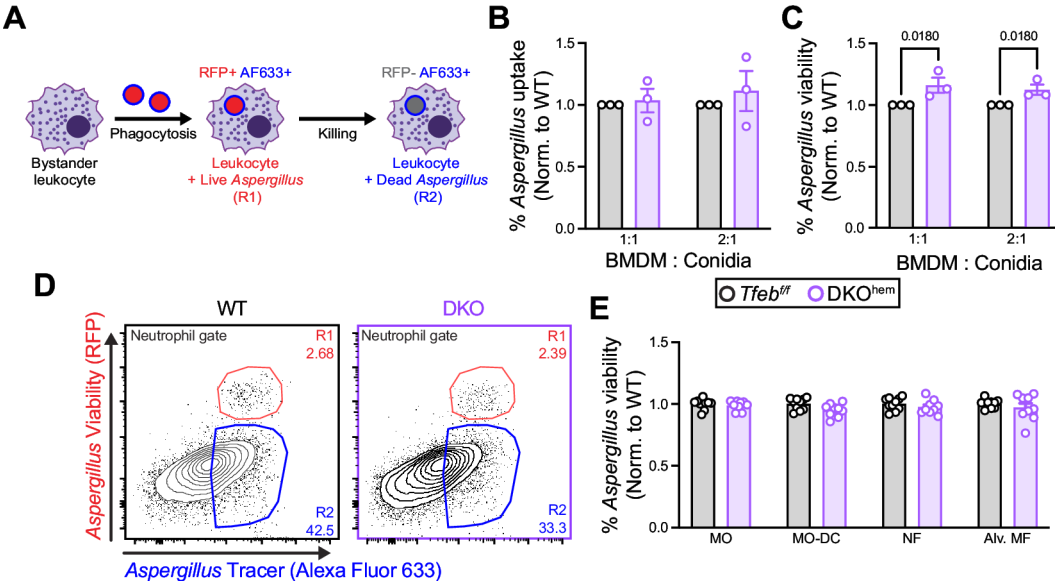

FIG 3 TFEB and TFE3 promote the killing of *A. fumigatus in vitro* but not *in vivo*. (A) Schematic of FLARE strain and changes in fluorescence emission following fungal uptake and killing by host phagocytes. (B) The plots show *Aspergillus* uptake (R1 + R2) ± SEM and (**C**) *Aspergillus* viability (R1/(R1 + R2) ± SEM in BMDMs from DKO^{hem} (purple) and *Tfeb*$^{f/f}$ (black) mice after overnight co-culture with FLARE conidia at the indicated ratios. (D) Representative plots that display RFP and AF633 fluorescence intensity of lung neutrophils in Tfeb$^{f/f}$ (left panel) or DKO^{hem} (right panel) 24 hpi with 3×10^7 CEA10 FLARE conidia. (E) The plots show conidial viability in monocytes (MO), Mo-DCs, neutrophils (NF), and alveolar macrophages (Alv. MF) isolated from DKO^{hem} (purple) and *Tfeb*$^{f/f}$ (black) 24 hpi with 3×10^7 FLARE conidia. (B, C, and E) Data from (B and C) three or (E) two experiments were pooled. (B, C, and E) Dots represent individual mice and data are expressed as mean ± SEM. Statistics: two-way ANOVA with Sidak's multiple comparisons test.

the uptake of conidia between DKO^{hem} and *Tfeb*$^{f/f}$ BMDMs (Fig. 3B), but we did observe a significant increase in the fraction of live conidia in DKO^{hem} compared to *Tfeb*$^{f/f}$ BMDMs (Fig. 3C). This finding indicates that genetic loss of TFEB and TFE3 impairs macrophage killing of *A. fumigatus in vitro*.

Given the defect in fungal killing we observed *in vitro* in DKO^{hem} macrophages, we hypothesized that TFEB and TFE3 would regulate phagocyte killing in the lung during *A. fumigatus* infection. To test this, we challenged DKO^{hem} or *Tfeb*$^{f/f}$ mice with FLARE conidia and at 24 hpi, we harvested the lungs and quantified the phagocytosis and killing of *A. fumigatus* by lung phagocytes as well as phagocyte numbers in the lung (see Fig. S3A and C for the details of gating strategy). DKO^{hem} mice had slightly greater numbers of lung monocytes and Mo-DCs but had no difference in alveolar macrophages or neutrophils compared to control mice (Fig. S3B). We observed no difference in the phagocytosis of *A. fumigatus* conidia by lung phagocytes in DKO^{hem} mice compared to *Tfeb*$^{f/f}$ (Fig. S3D), consistent with our *in vitro* findings (Fig. 3B). In contrast to *in vitro* results with BMDMs, DKO^{hem} lung phagocytes exhibited no defect in conidial killing (Fig. 3D and E) since the frequency of live fungal cells was similar in DKO^{hem} and control phagocytes for each phagocyte population analyzed. This result suggests that while TFEB and TFE3 promote the fungicidal activity of macrophages *in vitro*, their expression is dispensable for fungal killing by myeloid phagocytes *in vivo*.

Since fungal uptake led to an increase in LysoTracker staining in fungus-engaged myeloid cells compared to neighboring bystander cells (Fig. 1D), we next investigated whether this increase is regulated by TFEB and TFE3 gene function. To test this, we generated bone marrow chimeras with *Tfeb*$^{f/f}$ mice and DKO^{hem} mice with *A. fumigatus* and measured LysoTracker staining in lung single-cell populations by flow cytometry at 24 hpi. Fungus-engaged phagocytes isolated from DKO^{hem} mice and *Tfeb*$^{f/f}$ control mice showed an increase in LysoTracker staining compared to bystander phagocytes. Thus, the expression of TFEB and TFE3 was not required for the increase in LysoTracker staining observed with fungal cell uptake (Fig. S4A and B in the supplemental material). These data support the notion that loss of TFEB and TFE3 does not impair lysosomal acidification in response to fungal engagement *in vivo*, which may explain why myeloid phagocytes do not exhibit an impairment in fungal killing.

TFEB and TFE3 are dispensable for immunity to *A. fumigatus* in the lung

While the contributions of TFEB and TFE3 to immune function have been extensively studied *in vitro* and in non-vertebrate animal models (22, 28), data on the role of TFEB and TFE3 in experimental murine infection models, and in the context of fungal infections, are lacking. To test the requirement for TFEB and TFE3 in hematopoietic cells in host defense against *A. fumigatus,* we generated bone marrow chimeric mice, using *Tfeb*$^{\Delta hem}$, DKO^{hem}, or *Tfeb*$^{f/f}$ donor bone marrow injected intravenously into irradiated recipient mice. Bone marrow chimeric mice were rested for 6 weeks and subsequently challenged with *A. fumigatus* conidia *via* the intratracheal route. We also challenged global TFE3 KO and *Tfeb*$^{f/f}$ control mice in separate experiments. All genotypes of mice were resistant to infection with *A. fumigatus* (Fig. 4A through C). We also did not observe a significant difference in *A. fumigatus* lung fungal burden in any group at 24 hpi (Fig. 4D through F).

To extend these findings to mice with lifelong defects in *Tfeb* gene function, we repeated the survival experiment in non-chimeric *Tfeb*$^{f/f}$ and *Tfeb*$^{\Delta hem}$ mice and observed no difference in survival among these groups (Fig. S5). This result confirms that *Tfeb* gene function in hematopoietic cells is dispensable for *A. fumigatus* host defense and that bone marrow chimerism (i.e., acute loss of *Tfeb* gene function in adult recipient mice) does not alter murine survival in prior experiments. Due to limitations in mouse numbers, we were not able to conduct survival experiments in DKO^{hem} mice in a non-chimeric setting. Overall, these findings indicate that TFEB (in hematopoietic cells) and TFE3 (globally) are not essential for clearance of *Aspergillus* from the lung or for survival following infection.

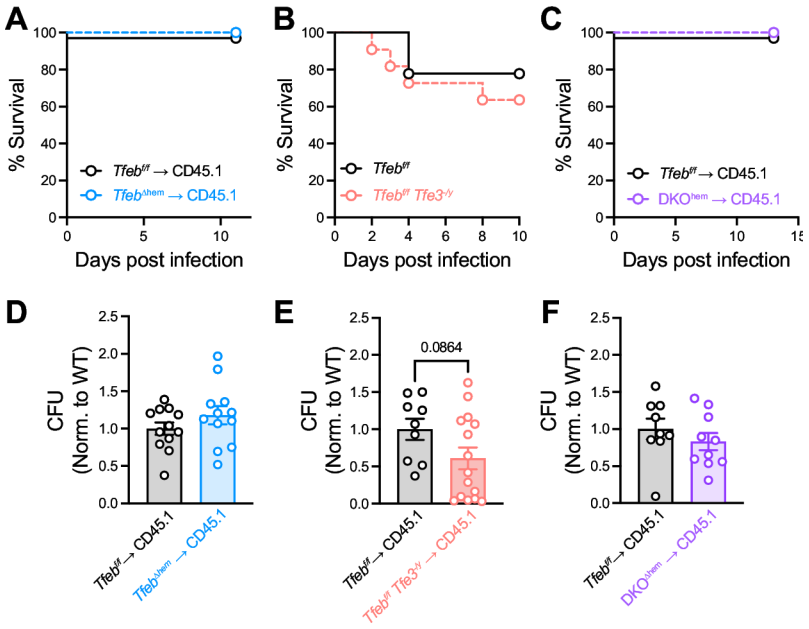

FIG 4 TFEB and TFE3 are dispensable for murine survival during *A. fumigatus* infection. (A–C) Kaplan-Meier survival curve of (A) *Tfeb*$^{f/f}$→ CD45.1 (n = 7) and *Tfeb*$^{\Delta hem}$→ CD45.1 (n = 8), (B) *Tfeb*$^{f/f}$ (n = 10) and *Tfeb*$^{f/f}$ *Tfe3*$^{-/y}$ (n = 11), and (C) *Tfeb*$^{f/f}$→ CD45.1 (n = 4) and DKO^{hem}→ CD45.1 (n = 6) hematopoietic chimera mice challenged with 6 × 10^7 CEA10 conidia. (D–F) Lung fungal burden at 24 hpi with 3 × 10^7 FLARE conidia in *Tfeb*$^{f/f}$→ CD45.1, *Tfeb*$^{\Delta hem}$→ CD45.1, *Tfeb*$^{f/f}$ *Tfe3*$^{-/y}$ → CD45.1, and DKO^{hem}→ CD45.1. (D–F) Data are pooled from two independent experiments and each dot indicates a mouse. Statistics: Mann-Whitney test.

DISCUSSION

This study aimed to investigate the role of transcription factors TFEB and TFE3 in phagocyte function during immune responses to *A. fumigatus*. We found that lysosome-related genes are upregulated in lung neutrophils following fungal engagement and that *A. fumigatus* conidia activate TFEB and TFE3 myeloid phagocytes, as determined by nuclear translocation. Activation of TFEB and TFE3 in response to *A. fumigatus* was impaired by deletion of Dectin-1 and CARD9, linking *Aspergillus* recognition to TFEB and TFE3 activation. In addition, *Tfeb* and *Tfe3* deletion in macrophages led to a reduction in fungicidal activity *in vitro*, although in the lung, no impairment in killing was observed. Interestingly, mice with hematopoietic TFEB deletion, TFE3 deletion, or combined deletion in the hematopoietic compartments were resistant to infection with *A. fumigatus*, indicating functional redundancy. Overall, this study provides valuable insights into the activation of TFEB and TFE3 in response to *A. fumigatus* conidia and the contribution of lysosome expansion to the effector functions of phagocytes upon fungal recognition. The study also adds to the growing literature on the role of TFEB and TFE3 in antifungal and antibacterial immunity.

Innate immune cells are known to employ various regulatory mechanisms upstream of TFEB and TFE3 to respond to pathogens. Phagocytosis of IgG-opsonized latex beads activates TFEB in macrophage-like RAW264.7 cells and primary BMDMs via FcγR and Syk (18). Syk is also a critical component of C-type lectin receptor signaling, linking Dectin-1 to Card9 (29). In response to *A. fumigatus*, Dectin-1 and Card9 are required for optimal activation of TFEB and TFE3, suggesting that Syk may also be involved in this context. Several groups have shown that calcium flux from the lysosome *via* MCOLN1 and activation of calcineurin are critical for the activation of TFEB and TFE3 in macrophages (18, 19) and other cell types (30). Fungal pathogen sensing *via* C-type lectin receptors can also trigger calcium flux in phagocytes (31). While we did not formally test the requirement for calcium and calcineurin, it is possible that these molecules are also

important for TFEB and TFE3 activation in response to *A. fumigatus*. Inhibition of mTOR also activates TFEB and TFE3 (32–34). However, it was recently shown that TFEB could be active in the context of hyperactive mTORC1 due to unique interactions between TFEB and Rag GTPases, suggesting that in specific settings, mTOR inhibition is not strictly required for TFEB and TFE3 activation (35). Since *A. fumigatus* is known to activate mTORC1 signaling in macrophages (36), fungus-induced TFEB and TFE3 activation likely occur in the presence of active mTORC1.

TFEB and TFE3 play important roles in the regulation of lysosome biogenesis and autophagy in various cell types, including macrophages (28). While overexpression of TFEB was found to increase lysosome biogenesis in murine macrophages (37), we did not observe significant differences in LysoTracker staining between TFEB and TFE3 knockout cells and wild-type cells, suggesting functional redundancy in lysosomal biogenesis and acidification in phagocytes during *A. fumigatus* infection. TFEB was also identified as a critical mediator of autophagy in *Mycobacterium tuberculosis*-infected macrophages (38). Multiple studies have demonstrated that *A. fumigatus*-containing phagosomes can recruit components of the autophagy pathway, including LC3 and Atg5, in a process described as LC3-associated phagocytosis (LAP) (39, 40). Deletion of key genes associated with LAP, such as *Rubicon* and *Atg5* in myeloid cells, delayed pulmonary *A. fumigatus* clearance (39, 40). Genetic loss of Atg5 in hematopoietic cells led to reduced survival in a cyclophosphamide model of invasive aspergillosis (39). We did not examine LC3 or *Atg5* induction in our BMDM or *in vivo* experiments.

LC3 recruitment to *A. fumigatus*-containing phagosomes is enhanced when phagocytes are challenged with a melanin-deficient strain (*ΔpksP*) and, conversely, is blocked by the addition of exogenous *A. fumigatus* melanin (39). Thus, melanin plays a key role in regulating autophagy induction in phagocytes during *A. fumigatus* challenge. By contrast, the finding that DKO^{hem} mice have normal pulmonary fungal clearance supports the idea that neither TFEB nor TFE3 is required for autophagy pathway function in response to *A. fumigatus* challenge. Beyond our analysis of the widely used CEA10 isolate, we did not assess whether strain-specific differences in melanin content or other virulence attributes impact the requirement for TFEB and TFE3 for *A. fumigatus* clearance.

TFEB and TFE3 were found to directly control the expression of several cytokines and chemokines in murine macrophages infected with pathogenic bacteria or stimulated with LPS (18, 21). While we did not measure TFEB- or TFE3-dependent lung cytokine levels, the lack of any defect in fungal clearance or differences in murine survival, suggests that it is thus unlikely that TFEB or TFE3 regulate the levels of essential mediators of intercellular crosstalk and host defense in the lung (e.g., GM-CSF (41), type I and type III interferon (42), or CXCL9 and CXCL10 (43)). It is possible that compensatory mechanisms exist to protect TFEB- and TFE3-deficient mice during infection, such as enhanced monocyte recruitment (Fig. S2). Neutrophils play a crucial role in anti-*Aspergillus* immunity and can compensate for the loss of alveolar macrophages during *A. fumigatus* infection (8). We observed a defect in the fungicidal activity of macrophages *in vitro* which suggested an essential role for TFEB and TFE3 in macrophage killing of *Aspergillus*. However, alveolar macrophages displayed no killing defect, suggesting that the lung inflammatory environment, including the fungicidal activity of neutrophils, may compensate for the loss of TFEB and TFE3-dependent macrophage killing activity. Our data do not exclude the possibility that TFEB and TFE3 may regulate fungal clearance in neutropenic or other severely immunocompromised models of disease.

In this study, we found that during *A. fumigatus* infection, phagocytes activate TFEB and TFE3 and expand their lysosomal compartment. While this pathway is activated *in vitro* and *in vivo* and is essential for optimal *A. fumigatus* conidiacidal activity *in vitro*, TFEB and TFE3 are ultimately not essential for murine survival during infection or for phagocyte function *in vivo*. This work contributes to our understanding of pathways that are activated in phagocytes upon *A. fumigatus* challenge and how lysosomes and TFEB and TFE3 contribute to phagocyte function.

MATERIALS AND METHODS

Mice

C57BL/6J mice (cat#: 000664) and *Vav-iCre* mice (cat#: 008610) were purchased from The Jackson Laboratory. CD45.1$^+$ C57BL6.SJL mice (cat#: 556) were purchased from Charles River Laboratories. *Tfeb$^{f/f}$* mice (34) were crossed with *Vav-iCre* mice to generate *Tfeb$^{\Delta hem}$*. *Tfeb$^{\Delta hem}$* mice were further crossed to *Tfe3$^{-/y}$* mice (44) to generate *Tfeb$^{\Delta hem}$ Tfe3$^{-/y}$* (DKO) mice. *Card9$^{-/-}$* mice (45) were provided by Dr. Xin Lin (Tsinghua University). *Clec7a$^{-/-}$* mice (46) were provided by Dr. Shinobu Saijo (University of Tokyo). All mouse strains were bred and housed in the MSKCC Research Animal Resource Center under specific pathogen-free conditions. All animal experiments were conducted with sex- and age-matched mice and performed with MSKCC Institutional Animal Care and Use Committee approval. Wherever possible, littermate controls were utilized. Animal studies complied with all applicable provisions established by the Animal Welfare Act and the Public Health Services Policy on the Humane Care and Use of Laboratory Animals.

Aspergillus fumigatus culture and murine infection model

A. fumigatus CEA10 (47) and CEA10-RFP (48) strains were cultured on glucose minimal medium slants at 37°C for 4–7 days prior to harvesting conidia for experimental use. To generate AF633-labeled or FLARE conidia for experimental use, 7×10^8 CEA10 (for AF633-labeled) or CEA10-RFP (for FLARE) conidia were rotated in 10 µg/mL Sulfo-NHS-LC-Biotin (Thermo Scientific) in 1 mL of 50 mM carbonate buffer (pH 8.3) for 2 hours at 4°C, incubated with 20 µg/mL Streptavidin, Alexa Fluor 633 conjugate (Molecular Probes) at 37°C for 1 hour, resuspended in phosphate-buffered saline (PBS) and 0.025% Tween 20 for use within 24 hours (12).

To generate morphologically uniform heat-killed swollen conidia, 5×10^6/mL conidia were incubated at 37°C for 14 hours in RPMI-1640 and 0.5 µg/mL voriconazole and heat-killed at 100°C for 30 minutes (49). To infect mice with 3–6 $\times$ 10^7 *A. fumigatus* cells, conidia were resuspended in PBS, 0.025% Tween-20 at a concentration of 0.6–1.2 $\times$ 10^9 cells/mL, and 50 µL of cell suspension was administered *via* the intratracheal route to mice anesthetized by isoflurane inhalation.

Transcriptomic analysis

Bystander and fungus-engaged neutrophils were sorted from the lungs of mice infected with AF633-labeled *A. fumigatus* conidia 24 hpi. Dead cells were excluded using DAPI (ThermoFisher cat#: EN62248). Bystander neutrophils were purified (>95% purity) by sorting as CD45$^+$, Ly6G$^+$, Ly6B$^+$, CD11b$^+$, and AF633$^-$ cells, and fungus-engaged neutrophils were purified (>95%) by sorting as CD45$^+$Ly6G$^+$, Ly6B$^+$, CD11b$^+$, and AF633$^+$ cells using a BD FACSAria cell sorter.

For RNA extraction, sorted cells were lysed in TRIzol Reagent (ThermoFisher catalog # 15596018) and phase separation was induced with chloroform. Neutrophil-derived RNA was precipitated with isopropanol and linear acrylamide, washed with 75% ethanol, and resuspended in 15 µL nuclease-free water. For transcriptome sequencing, after RiboGreen quantification and quality control by Agilent BioAnalyzer, 10 ng total RNA with RNA integrity numbers ranging from 8.8 to 9.5 underwent amplification using the SMART-Seq v4 Ultra Low Input RNA Kit (Clonetech catalog # 63488), with 12 cycles of amplification. Subsequently, 10 ng of amplified cDNA was used to prepare libraries with the KAPA Hyper Prep Kit (Kapa Biosystems KK8504) using 8 cycles of PCR. Samples were barcoded and run on a HiSeq 2500 in a PE50 run, using the TruSeq SBS Kit v4 (Illumina). An average of 42 million paired reads were generated per sample and the percentage of mRNA bases per sample ranged from 73% to 84%.

Statistical analysis of RNASeq data was performed by the MSKCC Bioinformatics Core. The output data (FASTQ files) were mapped to the target genome using the rnaStar aligner that maps reads on a genomic basis and resolves reads across splice junctions. The 2pass mapping method was used, in which the first mapping pass uses a list of

known annotated junctions from Ensembl. Novel junctions found in the first pass were then added to the known junctions and a second mapping pass was performed in which the Remove Noncanonical flag was used. After mapping, the output SAM files were post-processed using the PICARD tool AddOrReplaceReadGroups to add read groups, sort the files, and convert them to the compressed BAM format. The expression count matrix was then computed from the mapped reads using HTSeq (www-huber.embl.de/users/anders/HTSeq) and one of several possible gene model databases. The raw count matrix generated by HTSeq was then processed using the R/Bioconductor package DESeq (www-huber.embl.de/users/anders/DESeq) which was used to both normalize the full data set and analyze differential expression between sample groups.

LysoTracker staining

Total intracellular lysosomal content was measured using LysoTracker Green DND-26 (cat#: L7526). Briefly, single-cell lung suspensions were incubated in complete Dulbecco's modified Eagle medium (DMEM) with 50 nM LysoTracker at 37°C for 45 minutes according to the manufacturer's instruction. Cells were then stained with antibodies against surface markers as described below and analyzed by flow cytometry.

Immunofluorescence staining and imaging of TFEB and TFE3

iBMDMs (50) were cultured in DMEM containing 10% FBS, penecillin and streptomycin, L-glutamine, and HEPES. This media is referred to as complete DMEM below. Cells were passaged at 1:10 every 3 days. To assess the subcellular localization of TFEB or TFE3 in iBMDM cells, 5×10^5 cells were seeded into 12-well plates on top of coverslips in complete DMEM. Swollen heat-killed conidia (SHKC) were prepared as described above and 5×10^6 SHKC were added to the appropriate wells (multiplicity of infection = 10). Following stimulation, cells were fixed using 4% paraformaldehyde (PFA) in PBS and permeabilized with PBS containing 0.25% Triton X-100. Cells were then incubated with rabbit α-TFEB (1:1,000) (ThermoFisher cat#: 50–156-5746) or rabbit α-TFE3 (1:1,000) (ThermoFisher cat#: HPA023881) followed by incubation with goat anti-rabbit IgG AF488 (ThermoFisher cat#: A-11008). Finally, cells were counterstained with 1 µg/mL DAPI, mounted on slides with Mowiol 4–88 (ThermoFisher cat#: 47–590-4100GM), and imaged using a Leica TCS SP5 Confocal Microscope. Nuclear TFEB or TFE3 was calculated by outlining DAPI-positive structures and calculating the average TFEB or TFE3 staining intensity in each region, using Fiji (51). For all conditions 200–500 cells were quantified.

BMDM differentiation

Tibias and femurs were removed from euthanized mice of the indicated genotype, cut with scissors at each end, and centrifuged to harvest bone marrow cells, as previously described (52). Bone marrow cells underwent red blood cell lysis and were plated at 1×10^7 bone marrow cells per 10 cm dish in macrophage differentiation media consisting of DMEM + 20% fetal bovine serum +30% L-929 M-CSF conditioned +2 mM L-glutamine + Pen/Strep (all purchased from ThermoScientific). Plates were fed with 5 mL of additional macrophage differentiation media on day 3 of differentiation. Cell culture media was removed on day 7 and day 8 cultures. Cells were detached from non-treated plates with cold RPMI + 3 mM ethylenediamine tetraacetic acid (EDTA). To analyze conidia uptake and killing, FLARE conidia were co-cultured with BMDMs at the indicated ratios overnight in complete DMEM. For co-culture with *A. fumigatus*, 0.5 µg/mL voriconazole was added to the media. BMDMs were detached with cold RPMI containing 3 mM EDTA, transferred to a 96-well U-bottom plate, and washed twice with PBS + 0.5% bovine serum albumin (ThermoScientific cat#: BP9703100) +0.5 mM EDTA. DAPI (0.1 µg/mL) was added to cells immediately before being analyzed by flow cytometry.

Flow cytometric analysis of BMDMs and single-cell lung suspensions

Single-cell lung suspensions were prepared for flow cytometry as described in reference (53), with minor modifications. Briefly, perfused murine lungs were placed in a gentle MACS C tube and mechanically homogenized in 5 mL of PBS using a gentle MACS Octo Dissociator (Miltenyi Biotec). Lung cell suspensions were lysed of RBCs, enumerated, and stained with fluorophore-conjugated antibodies prior to flow cytometric analysis on a Beckman Coulter Cytoflex LX and analyzed with FlowJo version 10.8.1. Dead cells were excluded using LIVE/DEAD Fixable Aqua Dead Cell Stain (ThermoFisher cat#: L34957). The antibodies used are the following: anti-Ly6C (clone AL-21), anti-Ly6G (clone 1A8), anti-CD11b (clone M1/70), anti-CD11c (clone HL3), anti-CD45 (clone 30-F11), anti-I-A/I-E (clone M5/114.15.2), anti-Ly6B.2 (clone 7/4), and anti-Siglec-F (clone E50-2440) all from Biolegend and BD Biosciences. Alveolar macrophages were identified as $CD45^+$ $CD11c^+$ Siglec-F^+ cells, neutrophils were identified as $CD45^+$ $CD11b^+$ $Ly6G^+$ cells, inflammatory monocytes as $CD45^+$ $CD11b^+$ $CD11c^-$ $Ly6G^-$ $Ly6C^{hi}$ MHC-II- cells, and Mo-DCs as $CD45^+$ $CD11b^+$ $CD11c^+$ $Ly6G^-$ $Ly6C^{hi}$ MHC-II^+ cells. To analyze the lung fungal burden, perfused murine lungs were homogenized using a PowerGen 125 homogenizer (Fisher) in 2 mL PBS, 0.025% Tween-20, and plated on Sabouraud dextrose agar.

In data analyses for a given leukocyte subset, conidial uptake refers to the frequency of fungus-engaged leukocytes, that is, the sum of RFP^+AF633^+ and RFP^-AF633^+ leukocytes. Conidial viability within a specific leukocyte subset refers to the frequency of leukocytes that contain live conidia (RFP^+AF633^+) divided by the frequency of all fungus-engaged leukocytes (RFP^+AF633^+ and $mCherry^-AF633^+$).

Generation of bone marrow chimeric mice

For bone marrow chimeras, $CD45.1^+$ C57BL6.SJL recipients were lethally irradiated (900 cGy), reconstituted with 2–5 × 10^6 $CD45.2^+$ *Tfeb*$^{f/f}$, *Tfeb*$^{f/f}$ *Tfe3*$^{-/y}$, *Vav*$^{iCre/+}$ *Tfebf*$^{f/f}$, or *Vav*$^{iCre/+}$ *Tfeb*$^{f/f}$ *Tfe3*$^{-/y}$ donor bone marrow cells isolated from littermates. After bone marrow transplantation, recipient mice received 400 µg/mL enrofloxacin in drinking water for 21 days to prevent bacterial infections and rested for 6–8 weeks prior to experimental use.

Western blotting

BMDMs were lysed in lysis buffer (150 mM NaCl, 50 mM HEPES pH 7.4, 1 mM EDTA, 1% Nonidet P-40, protease inhibitors). Total cell lysates were subjected to SDS–PAGE and then blotted with the indicated antibodies.

Quantitative PCR analysis

For quantitative RT-PCR, BMDMs were stimulated with *A. fumigatus*, and RNA was extracted using TRIzol Reagent. cDNA was generated from RNA using the Applied Biosystems High-Capacity RNA-to-cDNA Kit (ThermoFisher cat#: 4387406), and qRT-PCR was performed on a StepOnePlus Real-Time PCR System (Applied Biosystems) using TaqMan Fast Advanced Master Mix and TaqMan Gene Expression Assays (ThermoFisher Scientific) *Atp6v1c1* (Mm00445925) and *Ctsb* (Mm01310506).

Quantification and statistical analysis

Data are representative of at least two independent experiments, as indicated. All results are expressed as mean (±SEM) unless stated otherwise. The Mann-Whitney test was used for comparisons of two groups unless noted otherwise. The Kruskal-Wallis test was used for multi-group comparisons unless noted otherwise. Survival data were analyzed by log-rank test. All statistical analyses were performed with GraphPad Prism software, v10.0.3.

Resource availability

Further information and requests for resources or reagents should be directed to the Lead Contact, Tobias M. Hohl (hohlt@mskcc.org).

Materials availability

The data sets generated for this study can be found in NCBI GEO, NCBI accession no. GSE233353.

ACKNOWLEDGMENTS

We thank all members of the Hohl laboratory for insightful discussions. We thank Anupam Jhingran for his help with generating the RNA-sequencing data. We thank Eric Chan for his help with microscope operation and image analysis.

The studies were supported by NIH grants P30 CA008748 (to MSKCC), R37 AI093808 (TMH), R01 AI139632 (TMH), F31 AI161996 (MAA), and F31 AI167511 (KAMM). The funders had no role in study design, data collection, and analysis, the decision to publish, or preparation of the manuscript. We acknowledge assistance from the MSKCC core facilities including Bioinformatics Core, Flow Cytometry Core Facility, Integrated Genomics Operation, and Molecular Cytology Core Facility.

Conceptualization, T.M.H. and M.A.A; Methodology, T.M.H.; Investigation, M.A.A., K.A.M.M, M.G., and N.S.; Writing—Original Draft, M.A.A. and T.M.H.; Writing—Review & Editing, M.A.A. and T.M.H.; Funding Acquisition, T.M.H. and M.A.A; Resources, A.B.

AUTHOR AFFILIATIONS

[1]Louis V. Gerstner Jr. Graduate School of Biomedical Sciences, Sloan Kettering Institute, Memorial Sloan Kettering Cancer Center, New York, New York, USA
[2]Koret School of Veterinary Medicine, The Robert H. Smith Faculty of Agriculture, Food and Environment, The Hebrew University of Jerusalem, Rehovot, Israel
[3]Infectious Disease Service, Department of Medicine, Memorial Hospital, New York, New York, USA
[4]Human Oncology and Pathogenesis Program, Memorial Sloan Kettering Cancer Center, New York, New York, USA
[5]Immunology and Microbial Pathogenesis Graduate Program, Weill Cornell Graduate School, New York, New York, USA
[6]Telethon Institute of Genetics and Medicine (TIGEM), Pozzuoli, Italy
[7]Medical Genetics Unit, Department of Medical and Translational Science, Federico II University, Naples, Italy
[8]Department of Molecular and Human Genetics, Baylor College of Medicine, Houston, Texas, USA

AUTHOR ORCIDs

Mariano A. Aufiero http://orcid.org/0000-0003-2462-438X
Tobias M. Hohl http://orcid.org/0000-0002-9097-5412

FUNDING

Funder	Grant(s)	Author(s)
HHS | NIH | National Institute of Allergy and Infectious Diseases (NIAID)	AI161996	Mariano A. Aufiero
HHS | NIH | National Institute of Allergy and Infectious Diseases (NIAID)	AI139632, AI093808	Tobias M. Hohl
HHS | NIH | National Institute of Allergy and Infectious Diseases (NIAID)	AI167511	Kathleen A. M. Mills

Funder	Grant(s)	Author(s)
HHS | NIH | National Cancer Institute (NCI)	P30 CA008748	Tobias M. Hohl

AUTHOR CONTRIBUTIONS

Mariano A. Aufiero, Conceptualization, Funding acquisition, Investigation, Methodology, Visualization, Writing – original draft, Writing – review and editing | Neta Shlezinger, Investigation | Mergim Gjonbalaj, Investigation | Kathleen A. M. Mills, Investigation | Andrea Ballabio, Resources | Tobias M. Hohl, Conceptualization, Funding acquisition, Project administration, Resources, Supervision, Writing – original draft, Writing – review and editing

ADDITIONAL FILES

The following material is available online.

Supplemental Material

Supplemental figure captions (IAI00217-23-s0001.docx). captions of Fig. S1 to S5.
Figure S1 (IAI00217-23-s0002.eps). Card9 is required for optimal TFE3 activation in BMDMs in response to *A. fumigatus*.
Figure S2 (IAI00217-23-s0003.eps). Deletion of TFEB in hematopoietic cells using Vav-iCre.
Figure S3 (IAI00217-23-s0004.eps). Gating strategy for lung FLARE experiments.
Figure S4 (IAI00217-23-s0005.eps). LysoTracker staining in lung phagocytes from DKOhem mice during A. fumigatus infection.
Figure S5 (IAI00217-23-s0006.eps). TFEB is dispensable for murine survival in non-chimeric mice.
Table S1 (IAI00217-23-s0007.doc). TFEB target genes upregulated in engaged lung neutrophils.

REFERENCES

1. World Health Organization (WHO). 2022. WHO fungal priority pathogens list to guide research, development and public health action
2. Latgé J-P, Chamilos G. 2019. *Aspergillus fumigatus* and aspergillosis in 2019. Clin Microbiol Rev 33:e00140-18. https://doi.org/10.1128/CMR.00140-18
3. Hahn-Ast C, Glasmacher A, Mückter S, Schmitz A, Kraemer A, Marklein G, Brossart P, von Lilienfeld-Toal M. 2010. Overall survival and fungal infection-related mortality in patients with invasive fungal infection and neutropenia after myelosuppressive chemotherapy in a tertiary care centre from 1995 to 2006. J Antimicrob Chemother 65:761–768. https://doi.org/10.1093/jac/dkp507
4. Nivoix Y, Velten M, Letscher-Bru V, Moghaddam A, Natarajan-Amé S, Fohrer C, Lioure B, Bilger K, Lutun P, Marcellin L, Launoy A, Freys G, Bergerat J-P, Herbrecht R. 2008. Factors associated with overall and attributable mortality in invasive aspergillosis. Clin Infect Dis 47:1176–1184. https://doi.org/10.1086/592255
5. Centers for Disease Control and Prevention (U.S.). 2019. Antibiotic resistance threats in the United States, 2019. centers for disease control and prevention (U.S.).
6. Brown GD, Denning DW, Gow NAR, Levitz SM, Netea MG, White TC. 2012. Hidden killers: human fungal infections. Sci Transl Med 4:165rv13. https://doi.org/10.1126/scitranslmed.3004404
7. Espinosa V, Jhingran A, Dutta O, Kasahara S, Donnelly R, Du P, Rosenfeld J, Leiner I, Chen C-C, Ron Y, Hohl TM, Rivera A. 2014. Inflammatory monocytes orchestrate innate antifungal immunity in the lung. PLoS Pathog 10:e1003940. https://doi.org/10.1371/journal.ppat.1003940
8. Mircescu MM, Lipuma L, van Rooijen N, Pamer EG, Hohl TM. 2009. Essential role for neutrophils but not alveolar macrophages at early time points following *Aspergillus fumigatus* infection. J Infect Dis 200:647–656. https://doi.org/10.1086/600380
9. Levin R, Grinstein S, Canton J. 2016. The life cycle of phagosomes: formation, maturation, and resolution. Immunol Rev 273:156–179. https://doi.org/10.1111/imr.12439
10. Brown GD. 2011. Innate antifungal immunity: the key role of phagocytes. Annu Rev Immunol 29:1–21. https://doi.org/10.1146/annurev-immunol-030409-101229
11. Ibrahim-Granet O, Philippe B, Boleti H, Boisvieux-Ulrich E, Grenet D, Stern M, Latgé JP. 2003. Phagocytosis and intracellular fate of *Aspergillus fumigatus* conidia in alveolar macrophages. Infect Immun 71:891–903. https://doi.org/10.1128/IAI.71.2.891-903.2003
12. Jhingran A, Mar KB, Kumasaka DK, Knoblaugh SE, Ngo LY, Segal BH, Iwakura Y, Lowell CA, Hamerman JA, Lin X, Hohl TM. 2012. Tracing conidial fate and measuring host cell antifungal activity using a reporter of microbial viability in the lung. Cell Rep 2:1762–1773. https://doi.org/10.1016/j.celrep.2012.10.026
13. Philippe B, Ibrahim-Granet O, Prévost MC, Gougerot-Pocidalo MA, Sanchez Perez M, Van der Meeren A, Latgé JP. 2003. Killing of *Aspergillus fumigatus* by alveolar macrophages is mediated by reactive oxidant intermediates. Infect Immun 71:3034–3042. https://doi.org/10.1128/IAI.71.6.3034-3042.2003
14. Ballabio A, Bonifacino JS. 2020. Lysosomes as dynamic regulators of cell and organismal homeostasis. Nat Rev Mol Cell Biol 21:101–118. https://doi.org/10.1038/s41580-019-0185-4
15. Martina JA, Diab HI, Lishu L, Jeong-A L, Patange S, Raben N, Puertollano R. 2014. The nutrient-responsive transcription factor TFE3 promotes autophagy, lysosomal biogenesis, and clearance of cellular debris. Sci Signal 7:ra9. https://doi.org/10.1126/scisignal.2004754
16. Sardiello M, Palmieri M, di Ronza A, Medina DL, Valenza M, Gennarino VA, Di Malta C, Donaudy F, Embrione V, Polishchuk RS, Banfi S, Parenti G, Cattaneo E, Ballabio A. 2009. A gene network regulating lysosomal

biogenesis and function. Science 325:473–477. https://doi.org/10.1126/science.1174447
17. Settembre C, Di Malta C, Polito VA, Garcia Arencibia M, Vetrini F, Erdin S, Erdin SU, Huynh T, Medina D, Colella P, Sardiello M, Rubinsztein DC, Ballabio A. 2011. TFEB links autophagy to lysosomal biogenesis. Science 332:1429–1433. https://doi.org/10.1126/science.1204592
18. Gray MA, Choy CH, Dayam RM, Ospina-Escobar E, Somerville A, Xiao X, Ferguson SM, Botelho RJ. 2016. Phagocytosis enhances lysosomal and bactericidal properties by activating the transcription factor TFEB. Curr Biol 26:1955–1964. https://doi.org/10.1016/j.cub.2016.05.070
19. Pastore N, Brady OA, Diab HI, Martina JA, Sun L, Huynh T, Lim J-A, Zare H, Raben N, Ballabio A, Puertollano R. 2016. TFEB and TFE3 cooperate in the regulation of the innate immune response in activated macrophages. Autophagy 12:1240–1258. https://doi.org/10.1080/15548627.2016.1179405
20. Westman J, Walpole GFW, Kasper L, Xue BY, Elshafee O, Hube B, Grinstein S. 2020. Lysosome fusion maintains phagosome integrity during fungal infection. Cell Host Microbe 28:798–812. https://doi.org/10.1016/j.chom.2020.09.004
21. Schuster E-M, Epple MW, Glaser KM, Mihlan M, Lucht K, Zimmermann JA, Bremser A, Polyzou A, Obier N, Cabezas-Wallscheid N, Trompouki E, Ballabio A, Vogel J, Buescher JM, Westermann AJ, Rambold AS. 2022. TFEB induces mitochondrial Itaconate synthesis to suppress bacterial growth in macrophages. Nat Metab 4:856–866. https://doi.org/10.1038/s42255-022-00605-w
22. Visvikis O, Ihuegbu N, Labed SA, Luhachack LG, Alves A-M, Wollenberg AC, Stuart LM, Stormo GD, Irazoqui JE. 2014. Innate host defense requires TFEB-mediated transcription of cytoprotective and antimicrobial genes. Immunity 40:896–909. https://doi.org/10.1016/j.immuni.2014.05.002
23. Raben N, Puertollano R. 2016. TFEB and TFE3: linking lysosomes to cellular adaptation to stress. Annu Rev Cell Dev Biol 32:255–278. https://doi.org/10.1146/annurev-cellbio-111315-125407
24. Settembre C, De Cegli R, Mansueto G, Saha PK, Vetrini F, Visvikis O, Huynh T, Carissimo A, Palmer D, Klisch TJ, Wollenberg AC, Di Bernardo D, Chan L, Irazoqui JE, Ballabio A. 2013. TFEB controls cellular lipid metabolism through a starvation-induced autoregulatory loop. Nat Cell Biol 15:647–658. https://doi.org/10.1038/ncb2718
25. Palmieri M, Impey S, Kang H, di Ronza A, Pelz C, Sardiello M, Ballabio A. 2011. Characterization of the CLEAR network reveals an integrated control of cellular clearance pathways. Hum Mol Genet 20:3852–3866. https://doi.org/10.1093/hmg/ddr306
26. Steingrímsson E, Tessarollo L, Reid SW, Jenkins NA, Copeland NG. 1998. The bHLH-zip transcription factor Tfeb is essential for placental vascularization. Development 125:4607–4616. https://doi.org/10.1242/dev.125.23.4607
27. Shlezinger N, Irmer H, Dhingra S, Beattie SR, Cramer RA, Braus GH, Sharon A, Hohl TM. 2017. Sterilizing immunity in the lung relies on targeting fungal apoptosis-like programmed cell death. Science 357:1037–1041. https://doi.org/10.1126/science.aan0365
28. Irazoqui JE. 2020. Key roles of MIT transcription factors in innate immunity and inflammation. Trends Immunol. 41:157–171. https://doi.org/10.1016/j.it.2019.12.003
29. Gross O, Poeck H, Bscheider M, Dostert C, Hannesschläger N, Endres S, Hartmann G, Tardivel A, Schweighoffer E, Tybulewicz V, Mocsai A, Tschopp J, Ruland J. 2009. Syk kinase signalling couples to the Nlrp3 inflammasome for anti-fungal host defence. Nature 459:433–436. https://doi.org/10.1038/nature07965
30. Medina DL, Di Paola S, Peluso I, Armani A, De Stefani D, Venditti R, Montefusco S, Scotto-Rosato A, Prezioso C, Forrester A, Settembre C, Wang W, Gao Q, Xu H, Sandri M, Rizzuto R, De Matteis MA, Ballabio A. 2015. Lysosomal calcium signaling regulates autophagy via calcineurin and TFEB. Nat Cell Biol 17:288–299. https://doi.org/10.1038/ncb3114
31. Goodridge HS, Simmons RM, Underhill DM. 2007. Dectin-1 stimulation by *Candida albicans* yeast or zymosan triggers NFAT activation in macrophages and dendritic cells. J Immunol 178:3107–3115. https://doi.org/10.4049/jimmunol.178.5.3107
32. Roczniak-Ferguson A, Petit CS, Froehlich F, Qian S, Ky J, Angarola B, Walther TC, Ferguson SM. 2012. The transcription factor TFEB links mTORC1 signaling to transcriptional control of lysosome homeostasis. Sci Signal 5:ra42. https://doi.org/10.1126/scisignal.2002790
33. Martina JA, Chen Y, Gucek M, Puertollano R. 2012. MTORC1 functions as a transcriptional regulator of autophagy by preventing nuclear transport of TFEB. Autophagy 8:903–914. https://doi.org/10.4161/auto.19653
34. Settembre C, Zoncu R, Medina DL, Vetrini F, Erdin S, Erdin S, Huynh T, Ferron M, Karsenty G, Vellard MC, Facchinetti V, Sabatini DM, Ballabio A. 2012. A lysosome-to-nucleus signalling mechanism senses and regulates the lysosome via mTOR and TFEB: self-regulation of the lysosome via mTOR and TFEB. EMBO J 31:1095–1108.
35. Napolitano G, Di Malta C, Esposito A, de Araujo MEG, Pece S, Bertalot G, Matarese M, Benedetti V, Zampelli A, Stasyk T, Siciliano D, Venuta A, Cesana M, Vilardo C, Nusco E, Monfregola J, Calcagnì A, Di Fiore PP, Huber LA, Ballabio A. 2020. A substrate-specific mTORC1 pathway underlies Birt–Hogg–Dubé syndrome. Nature 585:597–602. https://doi.org/10.1038/s41586-020-2444-0
36. Gonçalves SM, Duarte-Oliveira C, Campos CF, Aimanianda V, Ter Horst R, Leite L, Mercier T, Pereira P, Fernández-García M, Antunes D, Rodrigues CS, Barbosa-Matos C, Gaifem J, Mesquita I, Marques A, Osório NS, Torrado E, Rodrigues F, Costa S, Joosten LA, Lagrou K, Maertens J, Lacerda JF, Campos A Jr, Brown GD, Brakhage AA, Barbas C, Silvestre R, van de Veerdonk FL, Chamilos G, Netea MG, Latgé J-P, Cunha C, Carvalho A. 2020. Phagosomal removal of fungal melanin reprograms macrophage metabolism to promote antifungal immunity. Nat Commun 11:2282. https://doi.org/10.1038/s41467-020-16120-z
37. Sergin I, Evans TD, Zhang X, Bhattacharya S, Stokes CJ, Song E, Ali S, Dehestani B, Holloway KB, Micevych PS, Javaheri A, Crowley JR, Ballabio A, Schilling JD, Epelman S, Weihl CC, Diwan A, Fan D, Zayed MA, Razani B. 2017. Exploiting macrophage autophagy-lysosomal biogenesis as a therapy for atherosclerosis. Nat Commun 8:15750. https://doi.org/10.1038/ncomms15750
38. Ouimet M, Koster S, Sakowski E, Ramkhelawon B, van Solingen C, Oldebeken S, Karunakaran D, Portal-Celhay C, Sheedy FJ, Ray TD, Cecchini K, Zamore PD, Rayner KJ, Marcel YL, Philips JA, Moore KJ. 2016. *Mycobacterium tuberculosis* induces the miR-33 locus to reprogram autophagy and host lipid metabolism. Nat Immunol 17:677–686. https://doi.org/10.1038/ni.3434
39. Akoumianaki T, Kyrmizi I, Valsecchi I, Gresnigt MS, Samonis G, Drakos E, Boumpas D, Muszkieta L, Prevost M-C, Kontoyiannis DP, Chavakis T, Netea MG, van de Veerdonk FL, Brakhage AA, El-Benna J, Beauvais A, Latge J-P, Chamilos G. 2016. Aspergillus cell wall melanin blocks LC3-associated phagocytosis to promote pathogenicity. Cell Host Microbe 19:79–90. https://doi.org/10.1016/j.chom.2015.12.002
40. Martinez J, Malireddi RKS, Lu Q, Cunha LD, Pelletier S, Gingras S, Orchard R, Guan J-L, Tan H, Peng J, Kanneganti T-D, Virgin HW, Green DR. 2015. Molecular characterization of LC3-associated phagocytosis reveals distinct roles for rubicon, NOX2 and autophagy proteins. Nat Cell Biol 17:893–906. https://doi.org/10.1038/ncb3192
41. Kasahara S, Jhingran A, Dhingra S, Salem A, Cramer RA, Hohl TM. 2016. Role of granulocyte-macrophage colony-stimulating factor signaling in regulating neutrophil antifungal activity and the oxidative burst during respiratory fungal challenge. J Infect Dis 213:1289–1298. https://doi.org/10.1093/infdis/jiw054
42. Espinosa V, Dutta O, McElrath C, Du P, Chang Y-J, Cicciarelli B, Pitler A, Whitehead I, Obar JJ, Durbin JE, Kotenko SV, Rivera A. 2017. Type III interferon is a critical regulator of innate antifungal immunity. Sci Immunol 2:eaan5357. https://doi.org/10.1126/sciimmunol.aan5357
43. Guo Y, Kasahara S, Jhingran A, Tosini NL, Zhai B, Aufiero MA, Mills KAM, Gjonbalaj M, Espinosa V, Rivera A, Luster AD, Hohl TM. 2020. During *Aspergillus* infection, monocyte-derived DCs, neutrophils, and plasmacytoid DCs enhance innate immune defense through CXCR3-dependent crosstalk. Cell Host Microbe 28:104–116. https://doi.org/10.1016/j.chom.2020.05.002
44. Steingrimsson E, Tessarollo L, Pathak B, Hou L, Arnheiter H, Copeland NG, Jenkins NA. 2002. Mitf and Tfe3, two members of the Mitf-Tfe family of bHLH-zip transcription factors, have important but functionally redundant roles in osteoclast development. Proc Natl Acad Sci U S A 99:4477–4482. https://doi.org/10.1073/pnas.072071099
45. Hsu Y-M, Zhang Y, You Y, Wang D, Li H, Duramad O, Qin X-F, Dong C, Lin X. 2007. The adaptor protein CARD9 is required for innate immune responses to intracellular pathogens. Nat Immunol 8:198–205. https://doi.org/10.1038/ni1426
46. Saijo S, Fujikado N, Furuta T, Chung S, Kotaki H, Seki K, Sudo K, Akira S, Adachi Y, Ohno N, Kinjo T, Nakamura K, Kawakami K, Iwakura Y. 2007.

Dectin-1 is required for host defense against pneumocystis carinii but not against *Candida albicans*. Nat Immunol 8:39–46. https://doi.org/10.1038/ni1425
47. Girardin H, Latgé JP, Srikantha T, Morrow B, Soll DR. 1993. Development of DNA probes for fingerprinting *Aspergillus fumigatus*. J Clin Microbiol 31:1547–1554. https://doi.org/10.1128/jcm.31.6.1547-1554.1993
48. Liu K-W, Grau MS, Jones JT, Wang X, Vesely EM, James MR, Gutierrez-Perez C, Cramer RA, Obar JJ. 2022. Postinfluenza environment reduces *Aspergillus fumigatus* conidium clearance and facilitates invasive aspergillosis *in vivo*. mBio 13:e0285422. https://doi.org/10.1128/mbio.02854-22
49. Hohl TM, Van Epps HL, Rivera A, Morgan LA, Chen PL, Feldmesser M, Pamer EG. 2005. *Aspergillus fumigatus* triggers inflammatory responses by stage-specific β-glucan display. PLoS Pathog 1:e30. https://doi.org/10.1371/journal.ppat.0010030
50. Blasi E, Mathieson BJ, Varesio L, Cleveland JL, Borchert PA, Rapp UR. 1985. Selective immortalization of murine macrophages from fresh bone marrow by a raflmyc recombinant murine retrovirus. Nature 318:667–670. https://doi.org/10.1038/318667a0
51. Schindelin J, Arganda-Carreras I, Frise E, Kaynig V, Longair M, Pietzsch T, Preibisch S, Rueden C, Saalfeld S, Schmid B, Tinevez J-Y, White DJ, Hartenstein V, Eliceiri K, Tomancak P, Cardona A. 2012. Fiji: an open-source platform for biological-image analysis. Nat Methods 9:676–682. https://doi.org/10.1038/nmeth.2019
52. Amend SR, Valkenburg KC, Pienta KJ. 2016. Murine hind limb long bone dissection and bone marrow isolation. JoVE 53936. https://doi.org/10.3791/53936
53. Hohl TM, Rivera A, Lipuma L, Gallegos A, Shi C, Mack M, Pamer EG. 2009. Inflammatory monocytes facilitate adaptive CD4 T cell responses during respiratory fungal infection. Cell Host Microbe 6:470–481. https://doi.org/10.1016/j.chom.2009.10.007